International Journal of Fluid Power 7 (2006) No 1 pp. 15-25

MONITORING THE CONDITION OF A VALVE AND LINEAR ACTUATOR IN HYDRAULIC SYSTEMS

Jahmy J. Hindman [1], Richard Burton [2] and Greg Schoenau [2]

[1] *John Deere Construction & Forestry Division*
[2] *University of Saskatchewan, Mechanical Engineering Department*
HindmanJahmy@JohnDeere.com

Abstract

The topic of condition monitoring has been a growing area of research in both academia and industry for much of the last two decades. Condition monitoring of fluid power equipment has been no exception to this trend. Much of the research work associated with monitoring the condition of fluid power equipment has centered on pump and motor components due to their relatively high cost and complexity. The work in this paper focuses on the lesser expensive, but more common components of valves and linear actuators. The primary focus of the work presented here pertains to assessing the independent component condition of a valve-controlled linear actuator circuit. The paper first presents simulation studies to establish techniques for proper data collection, neural network training and output interpretation. The neural network approach is then applied to a valve and linear actuator of a John Deere 410E Backhoe Loader. The results indicate that the concept can be applied to a commercial system and is feasible for implementation.

Keywords: condition monitoring, neural network, valve, cylinder, actuator

1 Introduction

A significant amount of research has been conducted towards using parameter estimation techniques to monitor the condition of fluid power components. Several research projects on this topic have been pursued at the University of Saskatchewan in Canada. Cao (2001) uses the Extended Kalman Filter (EKF) algorithm to estimate parameters for both the swash plate assembly and control piston in a load-sensing pump. In this study, the damping coefficient, spring constant, and spring pretension in the assembly were estimated. Wright (2001) discusses using the EKF to estimate spring coefficients and precompressions, viscous friction, Coulomb friction, deadband and equivalent flow force spring coefficient in a proportional solenoid valve. Rosa (2001) utilizes an Artificial Neural Network (ANN) in estimating working parameters of the same proportional solenoid valve used by Wright (2001). The approach taken by Rosa utilized individual neuron structures to estimate each valve parameter. The main spool friction characteristics, orifice area gradient, main spool spring constant, and steady state flow force were all estimated using an ANN.

This manuscript was received on 16 August 2005 and was accepted after revision for publication on 25 January 2006

Watton et al. (1997) show the effectiveness of an ANN applied to detecting the leakages through an electro-hydraulic cylinder drive. A Multi-Layer Perceptron network architecture was adopted with six inputs, 50 nodes in the hidden layer and 31 outputs.

The 31 outputs were grouped into 4 separate categories. The first category was “Non-Leak”. The other three categories corresponded to either internal cylinder leakage, external cylinder leakage or both. There were 10 outputs for each of the latter three categories and one for the “Non-Leak” category. The 10 outputs for each of the leakage categories corresponded to a specified level of leakage.

Crowther et al. (1998) describe a network designed to detect three main actuator faults. The faults to be detected were a sudden decrease in supply pressure, an increase in external leakage, and an increase in the frictional characteristics of the load. Yunbo et al. (2001) discuss the results of using the root mean square of the vibration as measured from accelerometers to monitor the condition of an actuator and motor used in water hydraulic applications. A definite increase was seen in the vibration of the actuator as the piston seals wear. This was attributed to an increase in the rattling effect of the piston during extension and retraction as the

seals wear. Liang and Sepheri (2005) use the Extended Kalman Filter to successfully detect internal and external leakage in hydraulic actuators. A more detailed summary of the pertinent literature on this topic can be found in Hindman (2002). More general work on the topic can be found in Darling et al. (1993), Watton et al. (1996), Andrews et al. (1997), and Watton et al. (1994).

The valve controlled linear actuator is a very common circuit in modern hydraulic systems. These circuits are used in a variety of industries and applications ranging from off-highway construction equipment to control surface actuation in aerospace applications. Assessing the condition of the valve and actuator components that make up the circuit is a difficult task to accomplish. A critical component in monitoring the condition of these components is to determine the amount of internal leakage present within the components. This is a valid concern since internal leakage is related to the amount of wear present in the component. External leakage was not investigated in this research because external leakage is easily detectable through visual inspection of the mobile hydraulic system. The approach utilized in this research is to estimate the failure of each component due to the amount of internal leakage occurring in each component using a minimum of sensed information. In this research, the overall objective is to use pressure and temperature information to assess the condition of the valve and actuator by ultimately correlating that information to component wear by inference of internal leakage. This paper will first introduce the feasibility of the methodology to infer the wear from leakage information (via pressure) using simulation studies and an ANN. The second part of the paper will consider the experimental verification of the feasibility study. It should be noted that ANN's are not discussed in this paper as their usage is becoming commonplace in fluid power research and applications.

2 Simulation Study

2.1 Methodology

The method developed from this research work was derived from examining the behaviour of a direct operated, proportional, closed-center, over-lapped valve controlling a single linear actuator driven by a load sensing axial piston pump modeled in the Matlab Simulink® simulation environment. It should be noted here that the values of pressure, flow, clearances etc used in the simulation study, are those which typically can be found in off-road mobile equipment. Two distinct internal leakage paths were modeled in this simulation study (Hindman 2001). The first leakage path occurred between the valve spool and bore. The second leakage path occurred between the actuator seals and bore. These leakage paths can be seen in Fig. 1.

The annular leakage path produced by the geometry of these two components can be seen in Fig. 2. Due to the small magnitude of the clearances involved with the leakage paths, the flow around the annulus leakage path was assumed to be laminar. This assumption was validated by calculating the Reynold's number for the maximum leakage condition during the simulation. The laminar flow equation for the assumed leakage path is given in Eq. 1.

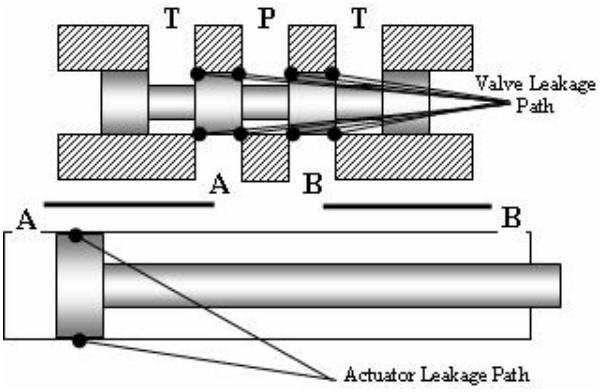

Fig. 1: *Modelled Leakage Paths*

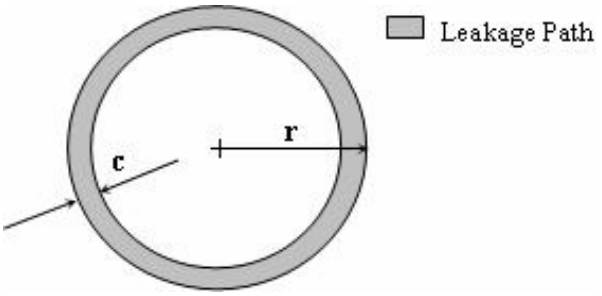

Fig. 2: *Annular Leakage Cross Section*

$$Q = \frac{\pi r c^3}{6\mu L}\left(P_1 - P_2\right) \tag{1}$$

where: r = Radius of bore (mm)

- c = Radial clearance between rod and bore (mm)
- μ = Absolute fluid viscosity (N-s/m^2)
- P_1 = Upstream pressure (Pa)
- P_2 = Downstream pressure (Pa)
- L = Length of leakage passage (mm)

The linear actuator was assumed to be fully retracted and pressurized to 245 bar on the rod side prior to the valve spool being shifted to its null position. This operating condition was chosen because the end of stroke condition is easily repeatable and is tractable to off-highway mobile equipment systems. It should be noted that in systems with circuit relief valves on the head and rod side (A and B port respectively) of the actuator, this condition should be repeatable with the maximum pressure roughly equivalent to the circuit relief pressure setting. The pressure behavior on both the head and rod side of the actuator was monitored during the simulation for a range of assumed radial clearance values. Leakage through the assumed circuit relief valve was assumed to be negligible. The results of this effort defined four different leakage regimes as illustrated in Fig. 3.

For the assumed actuator and valve, if the behavior of the rod and head side pressures is monitored for a sixty-second time interval, three critical pieces of in-

formation that assist in determining the magnitude and location (i.e. valve or actuator) of the internal leakage can be extracted. These three values are shown in Fig. 4. The three values shown in Fig. 4 are defined as:

1 Δt_1 = Time to achieve maximum change in rod-side pressure ± 35 kPa.
2 $\mathbf{\Delta P_1}$ = Maximum change in rod-side pressure over 60 second time interval.
3 $\mathbf{\Delta P_2}$ = Maximum change in head-side pressure over 60 second time interval.

The fourth and final piece of information necessary to completely characterize the magnitude and location of the internal leakage is the oil temperature (***T***). In this study, temperature is assumed constant but appears indirectly in the calculation of viscosity. The values of $\mathbf{\Delta P_1}$, $\mathbf{\Delta P_2}$, and $\mathbf{\Delta t_1}$ were calculated using the simulated closed center, over-lapped valve and actuator circuit for a range of radial valve and actuator clearances via Eq. 1. An external force was applied to the actuator when fully closed that held the actuator closed. This eliminated the actuator from drifting that may occur due to both cylinder and spool leakage when no force or a force of the opposite direction is applied (extension force). The results of this simulation effort are seen in Fig. 5.

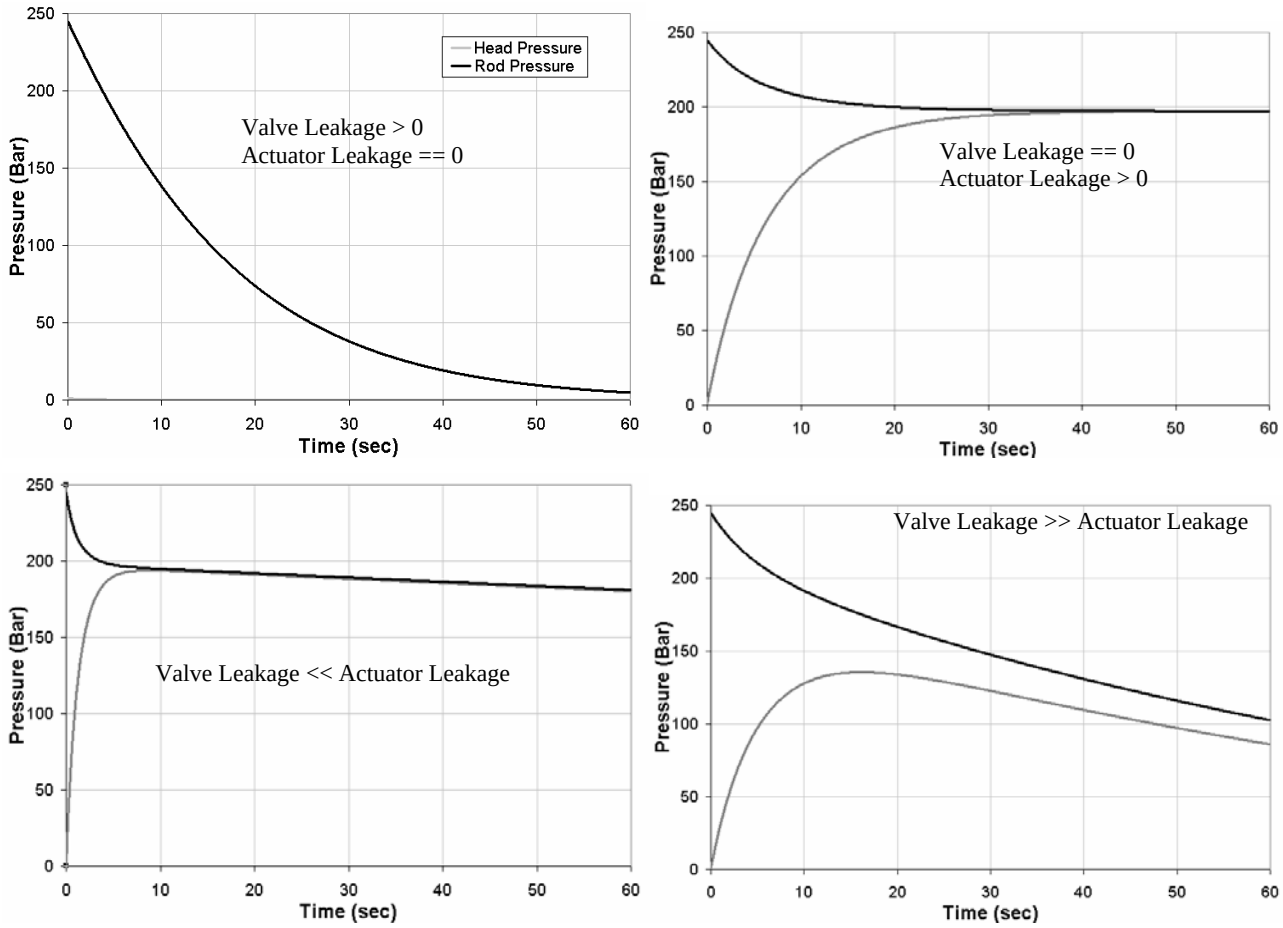

Fig. 3: *Leakage Regimes*

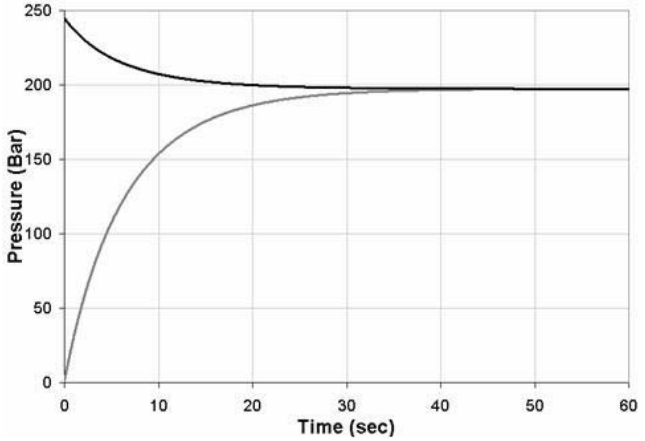

Fig. 4: *Critical Parameters*

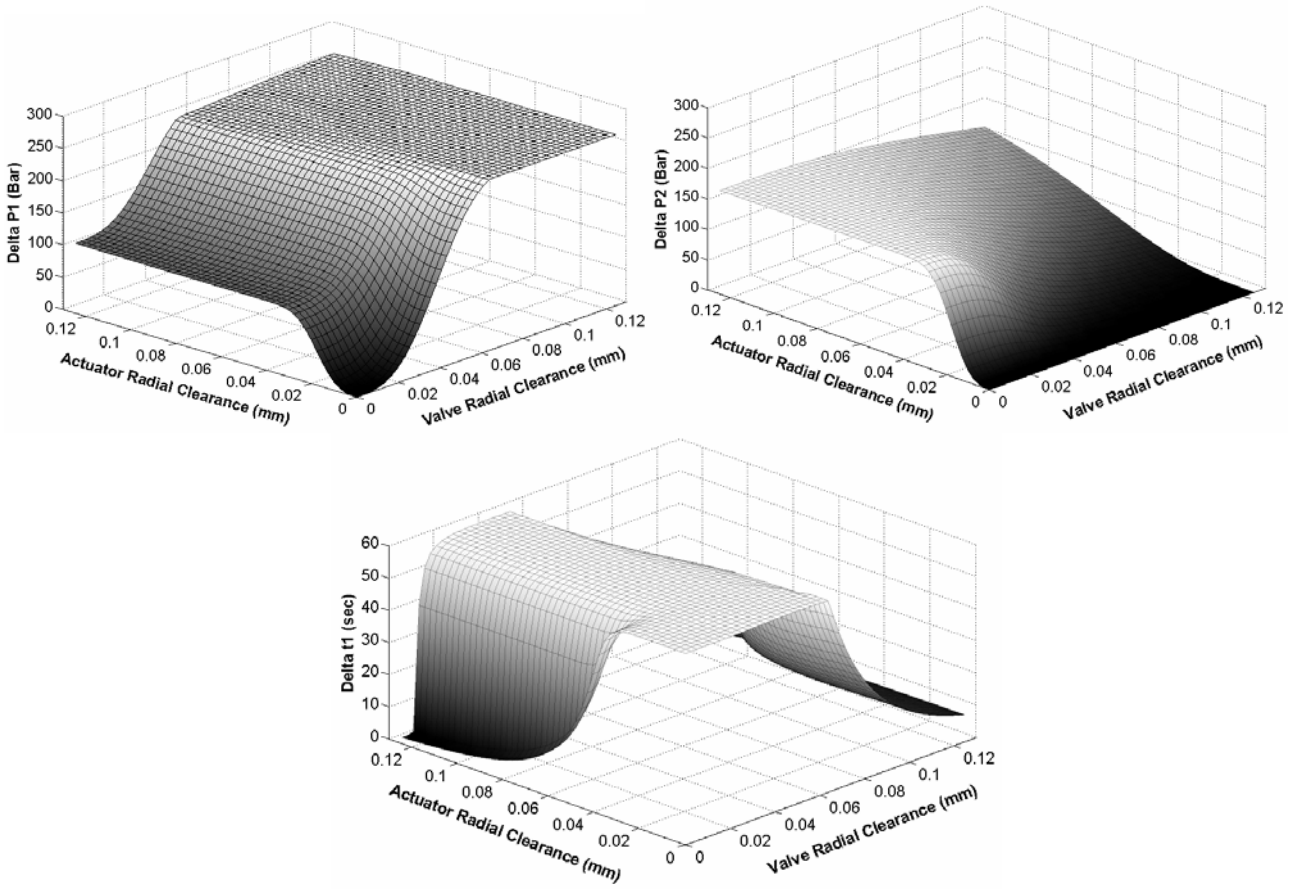

Fig. 5: *ΔP_1, ΔP_2, and Δt_1 as a Function of Actuator and Valve Clearance*

2.2 Simulation Results

Limits were imposed on the amount of internal leakage in the actuator and valve by limiting the amount of radial clearance allowed in each component. The limits are based on the typical machining and wear tolerances for these components in the mobile hydraulic application.

A linear mapping was then imposed that prescribed a percentage of actuator or valve "failure" to the amount of leakage as dictated by the radial clearance in each component. The 100% failure condition for the valve was equivalent to the largest radial clearance simulated in the valve. The 100% failure condition for the actuator was equivalent to the largest radial clearance simulated for the actuator. Zero radial clearance was equivalent to 0% failure with a linear rule applied between these two points. The three inputs of ΔP_1, ΔP_2, and Δt_1 at each data point were then mapped to these "failure" values through the use of a four layer (2x20x20x2) artificial neural network (ANN) assuming that temperature (T) was constant. This network was capable of mapping the input/output relationship to a high degree of accuracy and was trained using the Levenberg-Marquardt method (Hagan 1994). The results of the training process for the condition of the actuator and valve can be seen in Fig. 6.

By using the results of the 2000th epoch, the ANN was capable of learning the training data well enough to predict actuator failure within ± 0.68% damage and the valve failure (not shown) within ±0.41% damage assuming a 95% confidence interval (±2σ). This assumes that the inputs are known exactly with 100% confidence, which is a good assumption for the simulation results but will need to be revisited in the experimental work. Four input/output pairings were left out of the training data in order to test the trained network. These four conditions and the output of the trained ANN for these conditions are given in Table 1.

Using these four test cases, the trained ANN appears to be able to map the input pressure and time information to the expert data well. The average error in determining the actuator condition for these four cases is 2.0% of the known condition. The average error in determining the valve condition is 1.1% of the known condition. The ANN topology was determined by starting with training a very simple network and incrementally increasing network complexity until good generalization and accuracy were achieved. This provided the smallest network capable of generalizing well.

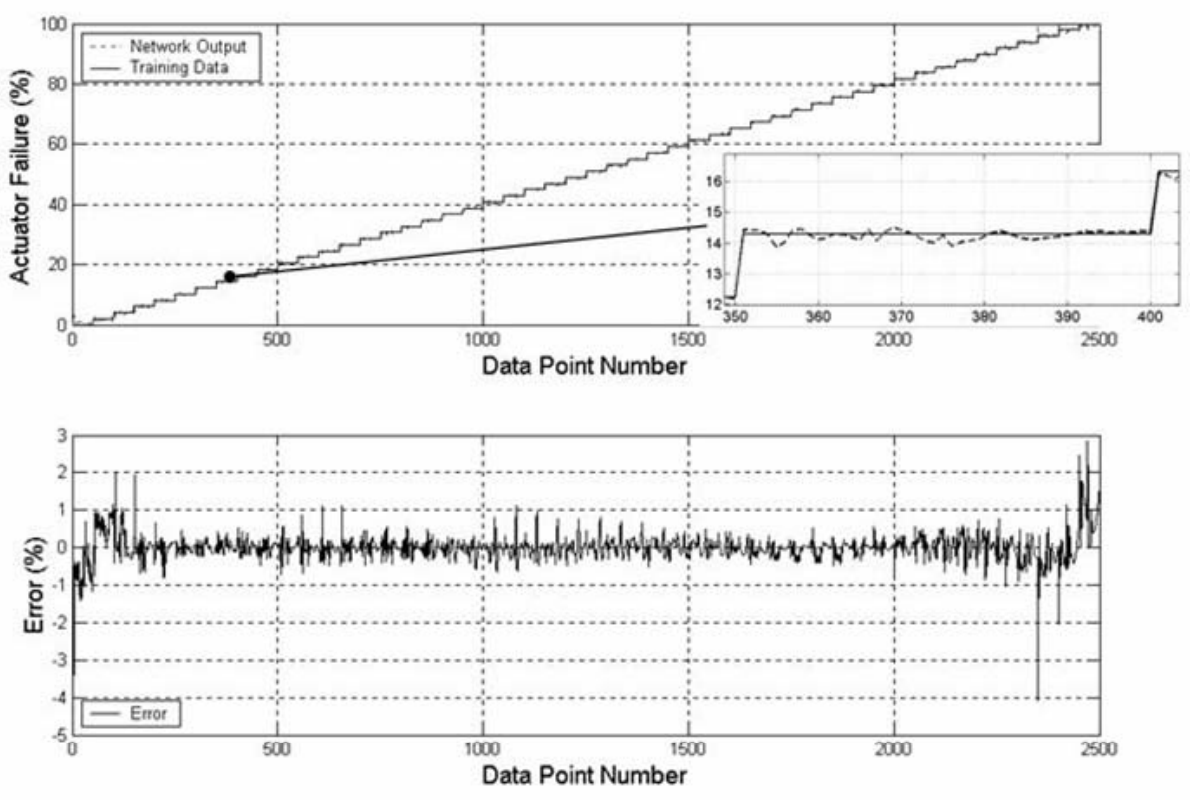

Fig. 6: *ANN Training using ΔP_1, ΔP_2, and Δt_1 as Inputs and Percentage Failure as Output*

Table 1: ANN Testing Results

ANN Input	Actuator Clearance (mm)	Desired Actuator Output	ANN Actuator Output	Actuator Error	Valve Clearance (mm)	Desired Valve Output	ANN Valve Output	Valve Error
ΔP_1=138 bar ΔP_2=115 bar Δt_1=60.0 sec	.028	22%	20.6%	*1.4%*	.028	22%	21.6%	*.4%*
ΔP_1=230 bar ΔP_2=153 bar Δt_1=60.0 sec	.083	66%	62.3%	*3.7%*	.048	38%	37.8%	*.2%*
ΔP_1=245 bar ΔP_2=.2 bar Δt_1=15.9 sec	.008	6%	7.1%	*1.1%*	.104	82%	79.6%	*2.4%*
ΔP_1=263 bar ΔP_2=115 bar Δt_1=57.4 sec	.064	50%	48.4%	*1.6%*	.064	50%	48.6%	*1.4%*

2.3 Simulation Discussion

The results of this study using simulated data indicate that the use of the ANN, with inputs of ΔP_1, ΔP_2, and Δt_1 can be used to predict the fault location (i.e. valve or actuator) and progression of leakage in a closed center valve and actuator. Due to the promise demonstrated by training an ANN with simulated data to characterize the leakage within the valve and actuator, it is now necessary to implement the concept using experimental data. It is expected that the complexity of the ANN topology for experimental implementation will be significantly greater than that for the simulation. This is due to the simulation assumption of constant fluid temperature. This assumption will be relaxed in the experimental implementation and thus the temperature becomes another input to the ANN. In addition, the experimental data will be subject to measurement and process noise that will lead to increased uncertainty in the ANN training data. The experimental results will be presented in Section 3.

As a final comment, the implementation of the required sensors to collect the input data is quite tractable. For every valve and actuator combination in the circuit, two pressure transducers and a single thermal sensor are required to be located between the valve and actuator. Depending upon the observed hydraulic oil temperature variation in the circuit, a single temperature measurement may suffice for several valve and actuator combinations. These sensors may be in addition to existing system sensors, or perhaps may already be implemented for system control purposes. This enables the economics of system implementation to be reasonable. The size of the machine utilizing this system and the machine's sen-

sitivity to down time and safety considerations assist in determining whether the system is implemented with on-board or off-board computational resources.

3 Experimental Considerations

Original Equipment Manufacturer (OEM) interest in condition monitoring of off-highway equipment (mining, construction and forestry) has increased significantly in the last several years due to increased customer focus on machine reliability and "uptime". The introduction of on-board computational ability has also enabled the implementation of condition monitoring algorithms to become a reality in these types of machines.

3.1 Methodology

The method developed from this research work was derived from examining the behaviour of a closed-center valve controlling a single linear actuator driven by a load sensing axial piston pump modeled in the Matlab Simulink® simulation environment. Two distinct internal leakage paths were modeled in this simulation study (Hindman 2001). The first leakage path occurred between the valve spool and bore. The second leakage path occurred between the actuator seals and bore. These leakage paths were illustrated in Fig. 1. The methodology developed from the simulation study in Section 1 was implemented experimentally on the boom cylinder and boom valve section in a John Deere 410E Backhoe Loader as seen in Fig. 7.

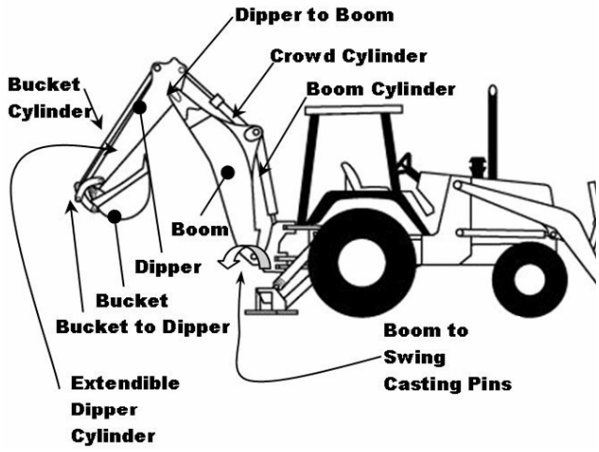

Fig. 7: *Backhoe Loader*

This machine utilizes the same direct operated, closed center, over lapped valve and load sensing pump as assumed in the simulation efforts. Several attempts were made to artificially introduce controlled leakage paths into the system for the internal and external leakage. The first attempt utilized small capacity variable needle valves. Two valves were located on the rod and head-side of the actuator (A) and the other was located in a line that shorted the head and rod-side actuator ports (B). This is illustrated in Fig. 8.

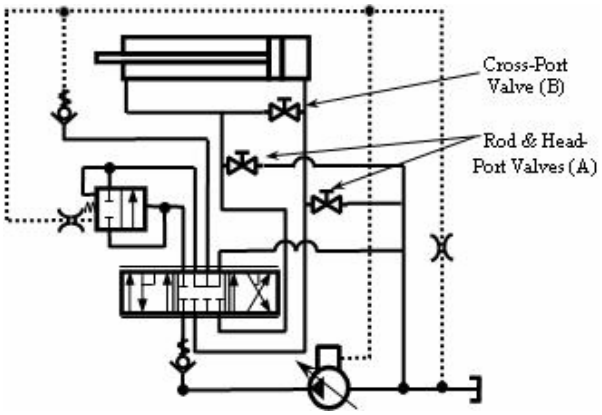

Fig. 8: *Valve Placement*

The cross-port valve simulates actuator seal leakage. The rod and head port valves simulate leakage occurring across the valve. These head and rod port valves are always set to the same opening assuming the valve spool wears similarly on the meter-in side as the meter-out side.

The large pressure drop (~ 28MPa) across the needle valves that occurred when the rod-side was fully pressurized prevented these valves from being used. This was due to the requirements for actuator and valve leakage to be extremely small in magnitude and the flow gain of the small needle valves being too large. Actuator drift of 3.05 mm per minute at an oil temperature of 60°C is used as the maximum allowable drift within this circuit. The drift requirement has been fixed from expert knowledge of what is allowable in the construction equipment marketplace. This actuator drift requirement translates to very small amounts of leakage, which were impossible to achieve with the needle valves in any repeatable manner due to the large pressure drop across the valve. It should be noted a significant distinction exists between the simulated model assuming a large force prohibiting the actuator from drifting and the actual backhoe boom cylinder which exhibits an extending force at all times due to the mass of the linkage always acting to extend the cylinder.

The second attempt at introducing controlled leakage to the system was to install very small (.33mm diameter) orifices downstream from the needle valves in an attempt to reduce the pressure drop across the needle valves. A smaller pressure drop across the needle valves increased their flow sensitivity, but was not sufficient in metering the required flow rates in a repeatable fashion.

The final configuration used to introduce the required leakage paths was a series of fixed diameter micro-orifices. The orifices ranged from .025 to .25 mm in diameter in increments of .025 mm. Three sets of these micro-orifices replaced the needle valves. This approach provided two advantages over using the needle valves. The first was the orifices in this size range were capable of metering the very small flow rates required for this experiment. The second advantage was that since the orifice size was fixed, the measurements were highly repeatable. The disadvantage of using these fixed orifices was that a different orifice needed to be used for every successive increment in leakage

rate compared to simply adjusting (though not repeatedly) the needle valve in the previous configuration.

To expedite the data collection phase, the small orifices simulating external leakage were installed in a manifold. A system schematic of the 410E boom circuit with these manifolds installed is shown in Fig. 10. Each orifice was turned on and off by means of a needle valve. This eliminated the need to disassemble the hydraulic lines to replace an orifice when a different leakage flow rate was desired. Fig. 9 shows the experimental configuration of the manifolds and orifices. The additional oil volume added by the manifolds and test plumbing was designed to be less than .5% of the dead volume of the head side of the actuator.

3.2 Experimental Procedure

The procedure described in Section 2.2 was used to obtain the experimental data necessary for training the ANN. Data was collected at oil temperatures in the range of 25°C to 45°C. The data collection process started with no artificial leakage present within the system (no artificially induced leakage paths). This condition represents "perfect" component health. This condition was repeated at the end of the experiment as well to ensure no significant unknown leakage was introduced during the experiment. The smallest orifice (.025 mm) was then used on the external leakage path, while no artificial leakage was introduced via the cross-port leakage path. The rod side of the actuator was pressurized with the main system pump, the spool returned to neutral, and the head and rod side pressure data acquired for sixty seconds. After the data was acquired, the orifice was replaced with the next larger size (.05 mm) and the procedure repeated. This continued until data was acquired with the largest orifice installed (.25 mm). At this point, the smallest orifice (.025 mm) was installed to provide an artificial cross-port leakage path. Data was again acquired for the complete range of orifices installed on the rod port. This process continued until data was acquired for all combinations of orifice sizes between the cross-port leakage and rod port leakage. There are 121 possible combinations of orifices (0 to .25mm in steps of .025mm = 11 sizes).

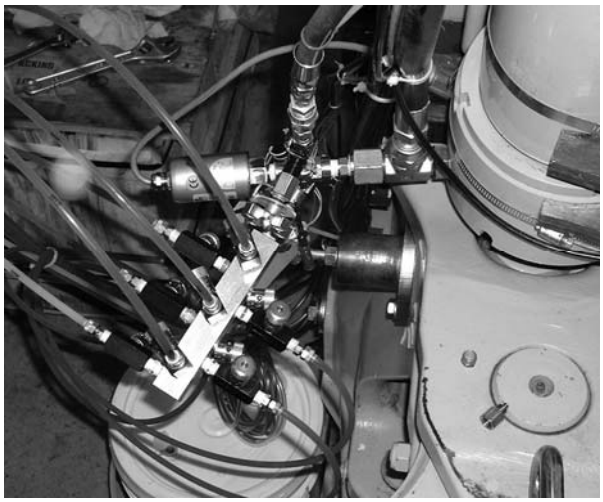

Fig. 9: *Orifice Configuration*

Since the temperature could not be maintained at a constant value, every effort was made to acquire data for a particular external/internal orifice configuration at different temperatures within the 25°C to 45°C temperature range. This was accomplished by taking four complete sets of data (for all orifice combinations) at various temperatures within the desired range. This provides ΔP_1, ΔP_2, Δt_1 and the amount of actuator drift at different oil temperatures for a given combination of external and internal leakage.

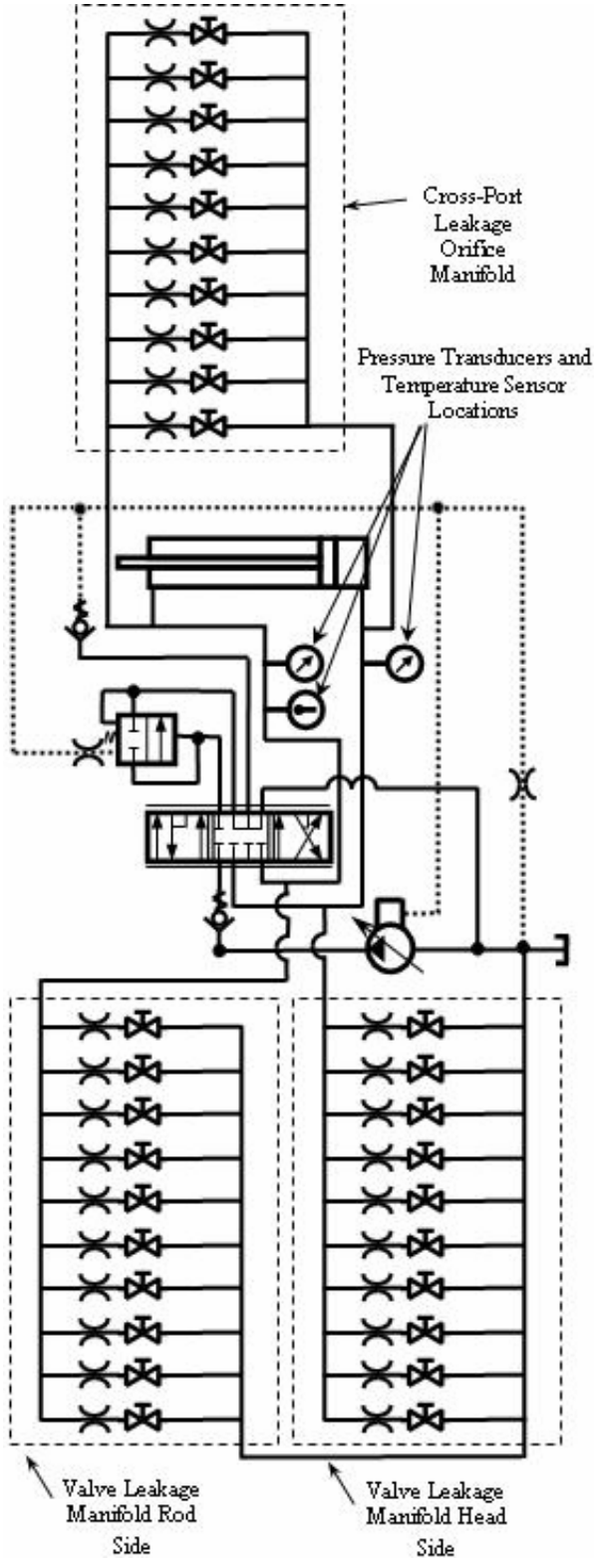

Fig. 10: *Experimental System Schematic*

3.3 Experimental Results

Once ΔP_1, ΔP_2, Δt_1 and the amount of actuator drift were acquired, the data was examined for spurious points and noise content. The measurements were quite clean as evidenced by the pressure trace shown in Fig. 11

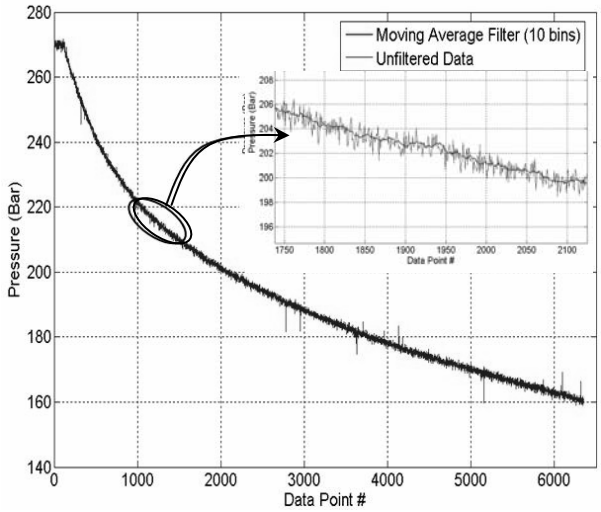

Fig. 11: *Sample Data*

In order to smooth the data and resolve any spurious points, a moving average filter was designed and implemented. The filter averaged ten time samples and used the average of the samples as the value for that time period. The length of the filter in this case was ten samples multiplied by the sampling rate of .01 seconds. The ten samples taken every .1 seconds were averaged. This filtering operation can be observed from Fig. 11 as well.

After filtering, ΔP_1, ΔP_2, Δt_1, oil temperature and the amount of actuator drift were extracted in order to train a neural network. The four inputs (ΔP_1, ΔP_2, Δt_1, oil temperature) are shown in Fig. 12.

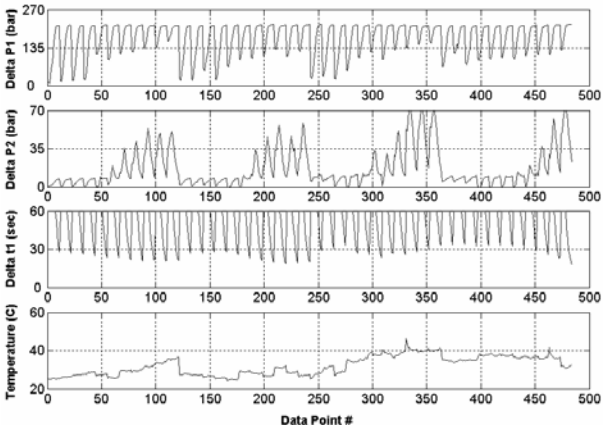

Fig. 12: *Typical Experimental Neural Network Inputs*

The outputs to the ANN were determined by comparing the measured actuator drift to the maximum drift allowed and determining the percentage of failure for each component (valve and actuator) based upon the orifice diameters that produced the actuator drift. It is worthwhile to clarify that the output of the ANN was not actuator drift, but an indicator of the progression of a fault based on a ratio of the measured and allowable drift. The maximum drift allowed is a function of oil viscosity (and thus temperature) and was determined from Eq. 2.

$$D_T = \frac{\mu_{ref}}{\mu_T}(.12) \tag{2}$$

where: μ_{ref} = oil viscosity at 60°C
μ_T = oil viscosity at desired oil temperature
D_T = allowable actuator drift (cm/min)

This equation is derived from expert system data that defines the maximum allowable actuator drift at 15.6 °C to be .35 cm/min.

The actuator drift obtained from the acquired data was then compared to the allowable actuator drift at the measured temperature for a complete set of all orifice combinations. This produces the data seen in Fig. 13, which will aid in the explanation of the how the neural network training outputs were arrived at.

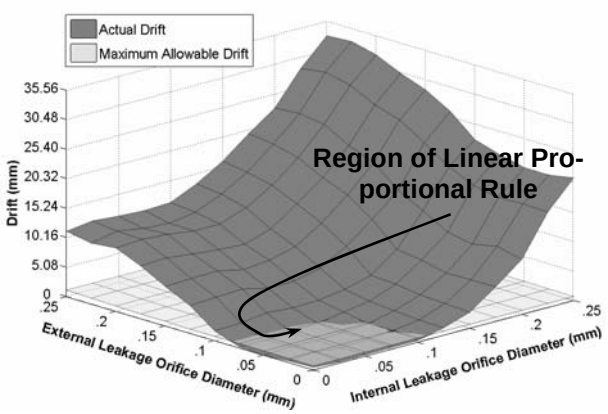

Fig. 13: *Actual and Allowable Actuator Drift, after 60 Seconds*

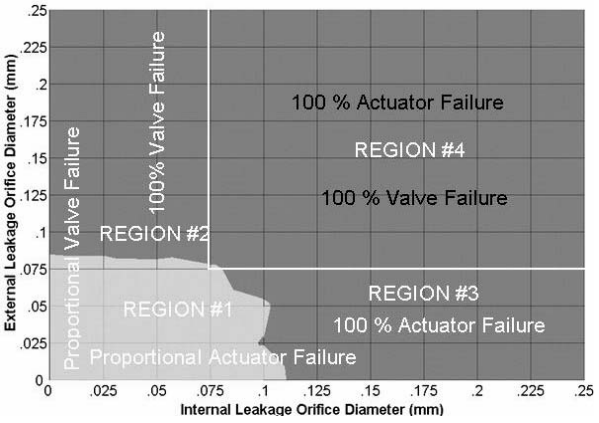

Fig. 14: *Top View Actual and Allowable Actuator Drift*

The output is determined by assuming a linear proportional damage "rule" within the area where the actual actuator drift is less than the allowable drift. This area is constrained by the intersection of the two surfaces shown in Fig. 13. If the actual actuator drift is greater than the allowable drift along either the internal or external orifice axis, the damage is 100% for the related component. It is important to remember that external leakage orifices correspond to valve failure and internal leakage orifices correspond to actuator

failure. The outputs of the ANN were trained to produce a measure of the degree of fault. Determination of the output is better illustrated by viewing Fig. 13 along the z-direction looking down on the two surfaces. This is illustrated in Fig. 14 in which the surfaces shown are not "flat" but contoured as in Fig. 13.

It is important to illustrate the method of determining the failure percentage based upon Fig. 13 with several examples. First consider the scenario where the external orifice diameter is .025 mm and the internal orifice diameter is .05 mm. Using this example, the valve failure is 30% (.025/.084). It is important not to forget that the external orifice is simulating the valve leakage. The failure attributed to the actuator is 50% (.05/.01). The internal orifice is simulating the actuator leakage. This same proportionality is used throughout Region #1 where the actual drift is less than the maximum allowable drift.

In regions where the actual drift is greater than the maximum allowable, but either one of the components is not completely failed (Regions 2 & 3), the component that is not completely failed is given a failure value proportional to the largest orifice that provided actuator drift less than the allowable drift in that component's direction. For example consider an external orifice diameter of .152 mm and an internal orifice diameter of .052 mm. The failure attributed to the valve is 100% (.152/.0765=200%→100% Failure). The failure attributed to the actuator should not be 100% however, since the excessive leakage in the valve is what is causing the large amount of actuator drift. In this case, the failure attributed to the actuator is 50% (.052/.104). This is determined by dividing the internal leakage orifice diameter by the largest internal orifice diameter that corresponds to the largest external orifice diameter that stays within the prescribed allowable drift (.104 mm).

An example of this calculation from Region 3 should be undertaken to assure understanding. Consider the external leakage orifice diameter of .051 mm and the internal leakage orifice diameter of .177 mm. This provides a valve failure of 66% (.051/.076) and an actuator failure of 100% (.177/.102=175%→100% Failure). All orifice combinations that fall within Region #4 are considered to be complete failure of both components.

This methodology to determine the predicted failure of the valve and actuator provides the outputs necessary to train an artificial neural network. The network that was chosen for training was a four layer feed-forward network with 10 neurons in the first layer, 15 in the second, 20 in the third, and two in the output layer (10x15x20x2). The four inputs of Fig. 12 were used to train the network coupled with the outputs generated by the methodology previously discussed. This network was batch1-trained with the Levenberg-Marquardt algorithm using 3500 epochs of data. All activation functions in this network were log-sigmoid functions. After training, the error was calculated by subtracting the desired output from the actual network output. The errors in the two outputs at the last iteration (3500) of batch training can be seen in Fig. 15.

It can be seen from Fig. 14 that the network trained to the input/output pairs to a high degree of accuracy. The performance of this network was deemed good enough to determine how well the network generalized. In order to determine this, the network was tested using inputs from data that was not used in the training process. It is important to remember that ΔP_1, ΔP_2, Δt_1 and the oil temperature are the inputs to the network and not the installed orifice diameters. That said, it is easier to intuitively understand the network output when the orifice diameters are known. Table 2 contains this information.

As can be seem from the table, the network generalizes well with the maximum error of 7% being shown for the cylinder prediction and 6 % for the valve. Further attempts could be made to construct a network that generalizes better, but that is not necessary for the "proof of concept" purposes outlined here.

3.4 Statistical Considerations

No experimental measurement is exact. Sensor resolution, signal noise and analog to digital conversion inaccuracy all play a part in diminishing the exactness of a measured signal. With this understood, it is important to determine how the neural network, trained and validated, responds when subjected to a likely *range* of data that statistically incorporates the disturbances mentioned above.In order to accomplish this, the standard deviation of the measured inputs is calculated for all of the input data collected. This provides the information seen in Table 3.

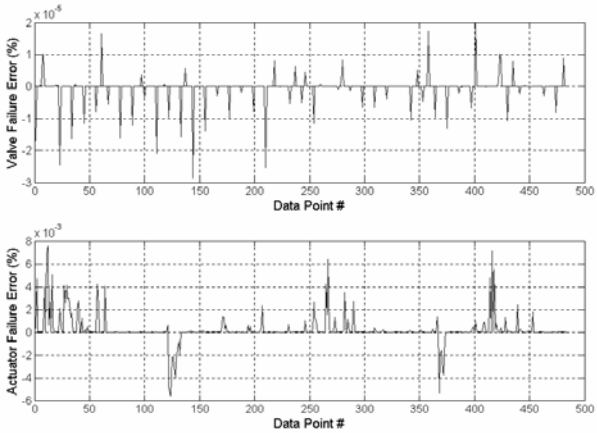

Fig. 15: *Neural Network Training Error (Experimental Data 3500th Epoch)*

In order to investigate the effect that a variation in the measurement parameter values about the mean (±2σ) has on the output of the network, the maximum and minimum of each input was applied to one input while using the median value for the other three. The maximum and minimum values were determined by adding or subtracting two standard deviations to the median value. This provides 95% confidence that any succeeding measurement will fall within the range bounded by this maximum and minimum. This is

1 "Batch" training simply means that all of the input/output pairs are presented to the network before the error is calculated and the weights changed accordingly.

termed the 95% Confidence Interval (C.I.). The best and worst case scenarios are seen in Table 4

It can be seen that the best accuracy that can be expected from the network with 95% confidence is ±1% (external orifice diameter of zero and internal orifice diameter of 9units) in addition to the ±6% network error shown in Table 2. The worst accuracy to be expected from the network is roughly ±8% in addition to the ±6% network error, as evidenced by the scenario where the external orifice diameter is .0762 mm and the internal orifice diameter is .2032 mm.

It is worthwhile to note that if low fidelity sensors are used to capture this data, the accuracy of the network will be diminished further than what is shown here due to the additional scatter induced by the sensor(s). Conversely, if a higher fidelity suite of sensors is utilized, the accuracy of the network may improve provided the network was retrained using data from the higher fidelity sensors. The accuracy of the results as obtained is generally acceptable to the off-highway industry.

4 Conclusions

This paper has considered the feasibility of using a neural network to establish the percent failure rate of an actuator and valve of a John Deere 410E Backhoe Loader. The simulation study was used to set up the procedures necessary to implement the approach and to establish the feasibility under ideal conditions.

The technique was applied to data collected from an actual unit and the data was then applied to a neural network. The results indicated that when testing data not used in the training process, the results were acceptable in terms of practical application. It was concluded that the approach is feasible both from a theoretical and applied point of view.

Table 2: Validation Information

Cross-Port Orifice Diameter (mm)	Head/Rod Orifice Diameter (mm)	Spool Condition (% Failure) Predicted | Actual	Cylinder Condition (% Failure) Predicted | Actual	Spool Condition Difference	Cylinder Condition Difference
.2032	0	.9% | 0%	100% | 100%	.9%	0%
.2032	.0229	79% | 73%	100% | 100%	6%	0%
.2032	.1016	94% | 95%	100% | 100%	1%	0%
.2032	.1524	100% | 100%	100% | 100%	0%	0%
.0508	.0508	2.2% | 5.1%	.01% | 2.7%	2.9%	2.6%
.0229	.0229	100% | 100%	82% | 76%	0%	6%
.0508	.1270	100% | 100%	73% | 67%	0%	6%
.1524	.0508	34% | 36%	100% | 100%	2%	0%

Table 3: Measurement Statistics

	ΔP_1 (psi)	ΔP_2 (psi)	Δt_1 (sec)	T (°C)
Standard Deviation (σ)	.66 bar	.71 bar	.63 sec	.14°
~95% C.I. (2σ)	1.31 bar	1.48 bar	1.26 sec	.28°

Table 4: Prediction Accuracy

	External Orifice Diameter (mm)	Internal Orifice Diameter (mm)	Mean Value Prediction (Valve Failure | Cylinder Failure)	Mean Value + 2σ Prediction	Mean Value - 2σ Prediction
$\Delta P_1 \pm 2\sigma$	0	.2286	.9% | 100%	1.9% | 100%	.4% | 100%
$\Delta P_2 \pm 2\sigma$	0	.2286	.9% | 100%	.6% | 100%	1.2% | 100%
$\Delta t_1 \pm 2\sigma$	0	.2286	.9% | 100%	.7% | 100%	1.1% | 100%
$T \pm 2\sigma$	0	.2286	.9% | 100%	.7% | 100%	1.1% | 100%
$\Delta P_1 \pm 2\sigma$	.0762	.2032	79% | 100%	87% | 100%	72% | 100%
$\Delta P_2 \pm 2\sigma$	.0762	.2032	79% | 100%	75% | 100%	83% | 100%
$\Delta t_1 \pm 2\sigma$	.0762	.2032	79% | 100%	87% | 100%	72% | 100%
$T \pm 2\sigma$	.0762	.2032	79% | 100%	73% | 100%	85% | 100%

Nomenclature

ΔP_1	Change in Pressure Rod Side	[bar]
ΔP_2	Change in Pressure Head Side	[bar]
Δt_1	Time to reach minimum pressure	[sec]
c	Radial clearance	[mm]
D_T	Allowable actuator drift	[cm/min]
L	Length of leakage passage	[mm]
P_1	Upstream pressure	[Pa]
P_2	Downstream pressure	[Pa]
r	Radius of bore	[mm]
μ	Absolute fluid viscosity	[N-s/m^2]

References

Andrews J. and **Henry J.** 1997. A computerised fault tree construction methodology. Proc IMechE, Part E, Journal of Process Mechanical Engineering. 211, 171-183.

Cao, H. 2001. Parameter Estimation Using Extended Kalman Filter for the Swash Plate Assembly and the Control Piston in a Load Sensing Pump. M.Sc.Thesis. University of Saskatchewan.

Crowther, W., **Edge, K.**, **Burrows, C.**, **Atkinson, R.** and **Woollons, D.** 1998. Fault diagnosis of a hydraulic actuator circuit using neural networks-an output vector space classification approach. Proc Instn Mech Engrs Vol. 212, Part I. pp. 57-69.

Darling R. and **Tilley D. G.** 1993. Progress towards a general purpose technique for the condition monitoring of fluid power systems. Proc IMechE Conference on Aerospace Hydraulics and Systems. London, 47-55.

Hagan, M. T. and **Menhaj, M.** 1994. Training Feed Forward Networks with the Marquardt Algorithm. IEEE Transactions on Neural Networks. Vol. 5(6). pp. 989-993.

Hindman, J. 2001. Condition Monitoring of Valves and Actuators in a Mobile Hydraulic System Using ANN and Expert Data. M.Sc. Thesis. University of Saskatchewan.

Hindman, J., **Burton, R.**, and **Schoenau, G.** 2002. Condition Monitoring of Fluid Power Systems: A Survey. SAE Journal of Commercial Vehicles, pp. 69-75.

Le, T., **Watton, J.** and **Pham, D.** 1997. An artificial neural network based approach to fault diagnosis and classification of fluid power systems. Proc Instn Mech Engrs Vol. 211, Part I. pp. 307-317.

Liang, A. and **Sepheri, N.** 2005. Hydraulic Actuator Leakage Fault Detection using Extended Kalman Filter, International Journal of Fluid Power,- FPNI, Vol. 6, Number 1, pp 41-52.

Rosa, A. 2001. Estimating Parameters of a Proportional Solenoid Valve using Neural Neworks. M.Sc. Thesis. University of Saskatchewan.

Watton J. and **Stewart J. C.** 1996. Co-operating expert knowledge and artificial neural networks for fault diagnosis of electrohydraulic cylinder position control systems. Proc 3rd JHPS International Symposium on Fluid Power. Yokohama. 217-222.

Watton J., **Lucca-Negro O.** and **Stewart J. C.** 1994. An on-line approach to fault diagnosis of fluid power cylinder drives systems. Proc IMechE Journal Systems and Control Engineering. Vol 208, 249-262.

Wright, G. 2001. Parameter Estimation of a Hydraulic Proportional Valve Using Extended Kalman Filtering. M.Sc. Thesis. University of Saskatchewan.

Yunbo, H., **Lim, G.**, **Chua, P.** and **Tan, A**. 2001. Monitoring the Condition of Loaded Modern Water Hydraulic Axial Piston Motor and Cylinder. Proceedings of the Fifth International Conference on Fluid Power Transmission and Control, pp. 447-451. Hangzhou, China.

Jahmy Hindman
Jahmy Hindman obtained his B.S. degree in mechanical engineering from Iowa State University in 1998. He obtained his M.Sc. degree in mechanical engineering from the University of Saskatchewan in 2002 where he is currently a PhD candidate. He is also the Engineering Supervisor of Hydraulics and Electrical groups for the John Deere Four-Wheel-Drive Loader group. His interests lie in hydraulic system design and control and artificial intelligence.

Richard Burton
Richard Burton received his PhD, and MSc degrees in Mechanical Engineering from the University of Saskatchewan. He is a professor of Mechanical Engineering at the University of Saskatchewan, has professional engineering status (P.Eng) with the Association of Professional Engineers of Saskatchewan and is a Fellow of ASME. Burton is involved in research pertaining to the application of intelligent theories to control and monitoring of hydraulics systems, component design, and system analysis.

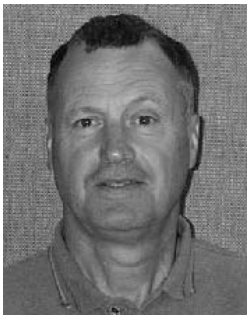

Greg Schoenau
Professor of Mechanical Engineering at the University of Saskatchewan. He was head of that Department from 1993 to 1999 and is now Associate Dean of Research. (2006). He obtained B.Sc. and M. Sc. Degrees from the University of Saskatchewan in mechanical engineering in 1967 and 1969, respectively. In 1974 he obtained his Ph.D. from the University of New Hampshire in fluid power control systems. He continues to be active in research in this area and in the thermal systems area as well. He has also held positions in numerous outside engineering and technical organizations.